Time-Series Clustering Analysis of Vegetation Indices Obtained from UAV to Visualize Fertilization Effect and High Temperature Influence

Taichi Ito[1,*,†], Ken'ichi Minamino[1,†] and Shintaro Umeki[2,†]

[1]Graduate School of Software and Information Science, Iwate Prefectural University, 152-52 Sugo, Takizawa-shi, Iwate, Japan
[2]Hanamaki Satellite, Research Center for Industrial Science and Technology, Iwate University, 5-6-3 Nimaibashi, Hanamaki-shi, Iwate, Japan

Abstract

2023 was the world's warmest year on record, summer 2023 in Japan, the high temperature reduced rice quality (i.e. the ratio of top-grade rice). The crop grades are directly linked to rice farmers' incomes. For stable production of high-quality crops, UAV monitoring whose introduction cost is reasonable, is attracting attention and expectations. In previous our research, time-series clustering analysis was developed on vegetation indices obtained from UAVs. In this research, the analysis method of previous research was applied to high-temperature years and analyzed changes in vegetation indices and additional fertilizer effects. As a result of time-series analysis, it was possible to determine which rice fields were fertilized appropriately. The fields diagnosed as adequate got the highest yields. In addition, although it was not at a statistically significant level, rice applied with chemical fertilizers had lower yields in high-temperature years than rice applied with organic fertilizers.

Keywords

high temperature, machine learning, drone monitoring, paddy rice, UAV, vegetation index

1. Introduction

Global warming has long become a problem, and the frequency of abnormal weather events is increasing. In Japan, heavy rain, heavy snow, and high temperatures occurred [1]. In particular, in 2023, the annual average temperature was the highest since 1946, when the Japan Meteorological Agency began keeping statistics [2]. In the case of paddy rice, high temperatures caused crops to grow faster, and farming work was moved forward by more than a week compared to usual years. The yield was 101% of the previous year because there was no shortage of temperature and sunlight. However, the ratio of top-grade rice (highest rank in coloration and traits) was approximately 17% lower than the previous year (Figure 1) [3, 4]. As the quality rank decreases, the transaction price also decreases, so it is important to produce high-yield and high-quality rice.

To produce high-quality crops, appropriate farming works are essential. On the other hand, previous research cited problems with Japanese farming work, such as "new workers cannot share expert farmers' tacit knowledge" and "it requires large human labor." In other words, the appropriate knowledge transfer and mechanization of farming works have not progressed. To solve these problems, Smart Agriculture has been proceeded such as production management systems [5]. However, the introducing and operating cost is enormous, and it has not become widespread in Japan, where there are many small and medium-sized individual farmers. Therefore, in the previous our research, Unmanned Aerial Vehicle (UAV) monitoring was adopted because it is more reasonable than other Smart Agricultural technologies. Also, it focused on additional fertilization and used machine learning to analyze Vegetation Index (VI) values obtained through continuous UAV monitoring. As a result, it clarified the growth of paddy rice

The 6th International Symposium on Advanced Technologies and Applications in the Internet of Things (ATAIT 2024), August 19-22, 2024, Kusatsu, Shiga, Japan
*Corresponding author.
†These authors contributed equally.
s236w001@s.iwate-pu.ac.jp (T. Ito); minamino@iwate-pu.ac.jp (K. Minamino); sumeki@iwate-u.ac.jp (S. Umeki)

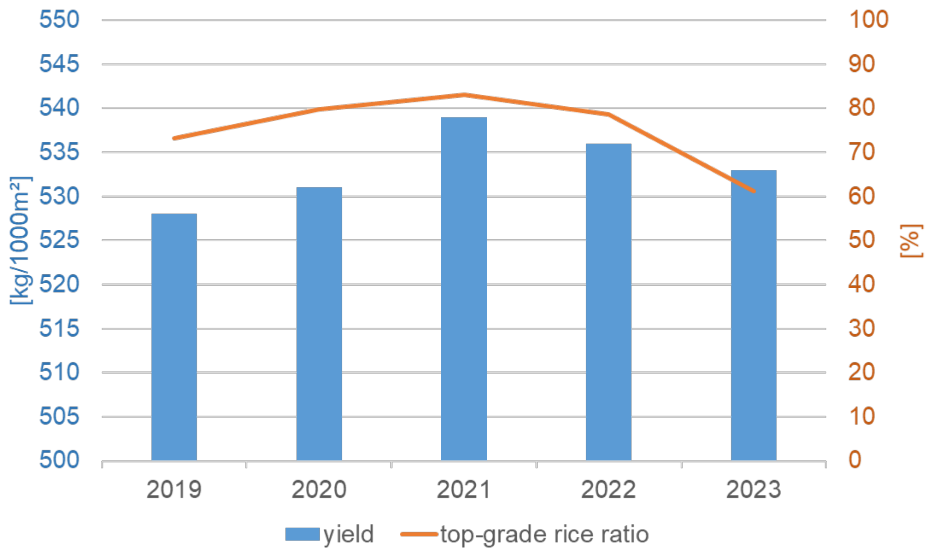

Figure 1: Average yield of paddy rice and the ratio of top-grade rice in Japan since

before and after additional fertilization, the appropriate amount of additional fertilizer, and the optimal monitoring period [6, 7]. Using the method, this paper visualizes the impact of high temperatures on paddy rice, and analyzes changes in vegetation indices and additional fertilizer effects to prevent high-temperature damage.

2. Method

2.1. Vegetation Index

This research used VI for remote monitoring of crops by UAV. VI uses the spectral reflectance of sunlight on plant leaves [8]. For example, the reflectance of stressed crops increases in the red band and decreases in the near-infrared band compared to healthy corps(Figure2) [9, 10]. VI is numerical vegetation using such reflection characteristics to understand crop condition from a formula. Various VI has been devised so far [11, 12]. By using such indicators, it is possible to diagnose yield, growth, and stress in paddy rice and wheat [13, 14, 15]. In this study, the following VIs were adopted to visualize the effect of fertilization and determine the amount of additional fertilizer needed for the experimental sites: the Normalized Difference Vegetation Index (NDVI) [13, 15, 16] and the Normalized Difference Red Edge Index (NDRE) [14, 17], which are used to diagnose the growth, yield, and stress. In addition, it was computed that the Standardized Normalized Difference Red Edge Index (SNDRE) [6, 7, 18], which are relative stress values for each day. The respective derivation formulas are (1), (2), and (3) below.

$$NDVI = (R_{NIR} - R_{Red})/(R_{NIR} - R_{Red}) \tag{1}$$

$$NDRE = (R_{NIR} - R_{RE})/(R_{NIR} - R_{RE}) \tag{2}$$

$$SNDRE = \left(NDRE - \mu^d_{NDRE}\right)/\sigma^d_{NDRE} \tag{3}$$

where

R_b :	Reflectance of band "b"
μ^d_{NDRE} :	Average of NDRE on date "d"
σ^d_{NDRE} :	Standard deviation of NDRE on date "d"

Monitoring was conducted at private farmer's paddy fields in Hanamaki City, Iwate Prefecture, Japan, from 2021 to 2023 at 6 sites in 10 conditions [6, 7, 18]. Among these monitoring sites, this paper deals

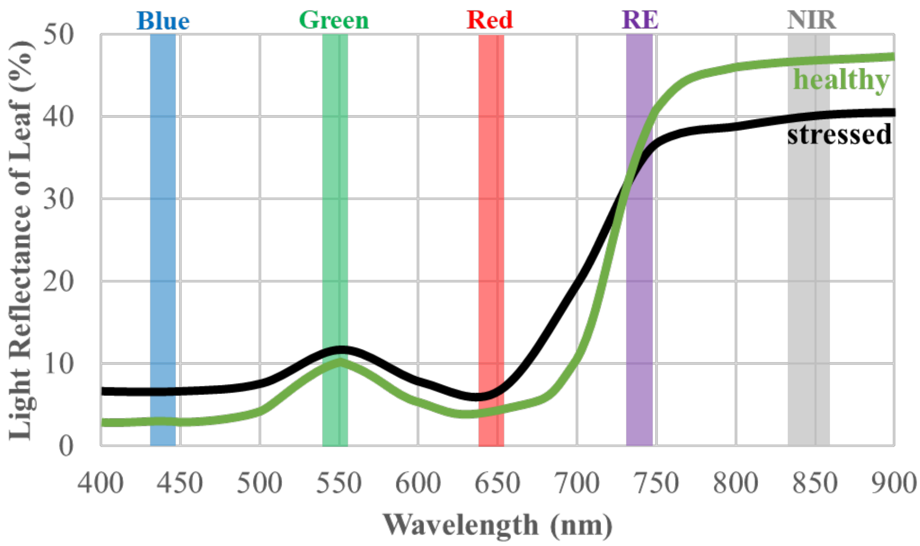

Figure 2: Image of spectral reflectance of plants [6, 7, 18]

Figure 3: UAV used in this study (DJI Ci., Ltd., China)

with the "Okamizawa" site, which was monitored in 2023 (high-temperature year). Table 1 shows growth information at Okamizawa. This site is divided into three fields (North, Center, and South), and the method of additional fertilization differs for each field. North field was used conventional chemical fertilizer. Center and South fields were fertilized with the farmers' homemade liquid fertilizer and organic cow dung. Note that preliminary analysis results of Time-Series Clustering (TSC) for this site have already been reported [19], this paper reports the results in detail.

The UAV used for monitoring is shown in Figure 3. This UAV is equipped with one RGB sensor for visible light and five monochrome sensors for multispectral. The bands of each monochrome sensor are 450nm (Blue), 560nm (Green), 650nm (Red), 730nm (RE: Red Edge), and 840nm (NIR: Near-Infrared) [20]. However, in this study, only the Red, RE, and NIR bands necessary for calculating NDVI and NDRE were used. To optimize the resolution of the drone images, camera settings were adjusted according to lighting conditions, distance, and drone speed (e.g. flight altitude: 30 meters). The monitoring interval was also set according to the growth stage (i.e. once a week from the panicle formation stage until before harvest). In addition, correcting errors in luminance values and coordinates, a standard reflector was used and 4 ground control points (GCP) were established at the four corners of the site. However, this period was the rainy season so there were missing measurements when drone flight was not possible.

Table 1
Growth information of the experimental field

Site	**Okamizawa**	
Comparative Experiment	Fertilization Method	
Number of Meshes	744	
Year	2022	2023
Rice Variety	Hitomebore	Yumi-azusa
Transplanting	May 7	May 5
Additional Fertilization	North Jul. 24 Center & South Aug. 1 Aug. 6	Same as in 2022 No date details available
Heading	Aug. 3	Late Jul.
Harvesting	Sep. 27	Mid-Sep.

2.2. Time-Series Analysis

In order to compute VI from aerial photographs taken by UAV, it is necessary to create orthophotos of each band. Therefore, they were generated using software (Agisoft Metashape, Agisoft LLC, Russia). Next, calculate NDVI, NDRE, and SNDRE from multiple orthophotos using free and open-source geographic information system (QGIS [21]). The VI value was calculated for each 3m square mesh. This was done on all observation days to create VI time-series data for each mesh. That is, there is VI time-series data for the number of meshes. These meshes were classified into several clusters according to the pattern of time-series changes in VI using a Python TSC program based on the K-Means++ method to [6, 7, 18]. Note that the number clusters were determined subjectively using the elbow method [22]. Using the VI time-series data at the centroid of each cluster and the cluster distribution map by this method, this paper will visualize the growth and stress of rice and diagnose which rice fields have been properly fertilized.

As an additional experiment from the previous research [19], a unit acreage sampling was conducted just before harvest. The sample method was to select 5 meshes from each rice field so that the NDVI values at the heading stage were dispersed, and then measure the yield of the 5 plants within each mesh. The selected meshes are shown in Figure 4. By the data of sample yield, the significant differences in yield between rice fields and which rice fields were most appropriately fertilized were evaluated.

3. Result

3.1. Fertilization Effect and High-Temperature Influence

As the results of TSC for Okamizawa, the time-series transitions of each cluster centroid and daily weather data are shown in Table 2. In addition, the cluster distribution map is shown in Table 3. The vertical dashed lines in each figure in Table 2 mean the growth stage transition dates. They were estimated from the growth stage prediction model based on the effective cumulative temperature from the date of transplantation [23, 24].

In 2022, a variety "Hitomebore" was planted which commonly consumed in Japanese households. As a comparative experiment, the fertilization method was changed for each rice field. In North field, chemical fertilizer was applied at 0.51g/m^2 of nitrogen equivalent on July 24th, and in Center and South fields, liquid fertilizer and cow dung were applied on August 1st and 6th [7]. Temperatures in the first half of June were approximately 3°C lower than normal, but other periods were around normal. A major feature was heavy rainfall in August, and the amount of solar radiation was approximately 70% of the normal. In NDVI, the cluster-ID appearing in each field was different. Based on reports that there is a correlation between NDVI and yield from the Panicle Formation stage to the Heading stage [16], the

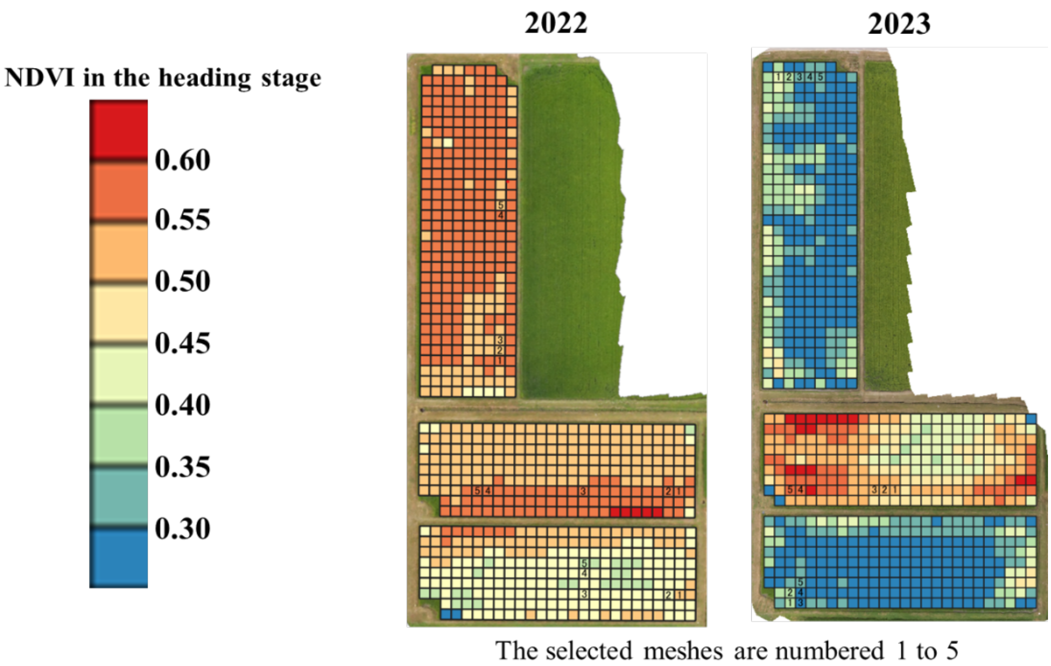

Figure 4: The meshes selected in unit acreage sampling

yield of North and Center field is expected to be higher. NDRE does not show much difference between clusters. Since NDRE value does not change unless a significant stress is imposed on plants [6, 7, 18], it is expected that there was no major stress at this site.

SNDRE was divided into Cluster-0 (large difference in fluctuation), Cluster-1(upward trend), Cluster-2(high values around the heading stage), and Cluster-3(fluctuation range between -0.5 and 0). Cluster-0 is an abnormal value because only a few meshes appear in the corner of the rice field. Cluster-1 was often seen near the ridges of each rice field, so it is thought that the fertilizer washed away by rain and wind was concentrated in these meshes. Cluster-2 appeared in North field and is thought that the effects of chemical fertilizers were evident. Cluster-3 appeared well in Center and South fields. It is thought that liquid fertilizer and cow dung were gradually absorbed into paddy rice over a longer time than chemical fertilizers. From these results, it is thought that the yield in North or Center field is higher, so these two fields were fertilized optimally.

In 2023, "Yumi-azusa" was planted. This variety has a lower taste than Hitomebore, but it is resistant to diseases. So, it is used as commercial rice. The comparative experiment will be roughly the same as in 2022, but detailed work dates were not recorded. Regarding the climate, the daily mean temperature was always higher than normal. In particular, it in August was approximately 4°C higher than normal. Additionally, the weather remained sunny before the heading stage, so there were few precipitations. In NDVI was divided into cluster-0 and cluster-1 (high values around the heading stage), and cluster-2 and cluster-3 (low values around the heading stage). Since high values clusters are often found in Center field, the yield would be higher. NDRE took a higher value compared to 2022. This meant lower stress levels so no growth problems were observed. In SNDRE, cluster-0 was high during the heading stage so it was a good transition that showed the effect of additional fertilizer. This cluster was found in Center fields. In any VIs, Center field was expected to be the best fertilization because well-diagnosed clusters are widely distributed in this field. But North and South fields were higher stress levels after the heading stage than Center field. Only Center field might have been less affected by high-temperature years.

Table 2: The centroid of each cluster and daily weather data (mean temperature, precipitation, and amount of solar radiation). Weather data is a 7-day centered moving average.

VI	2022	2023	Weather
NDVI	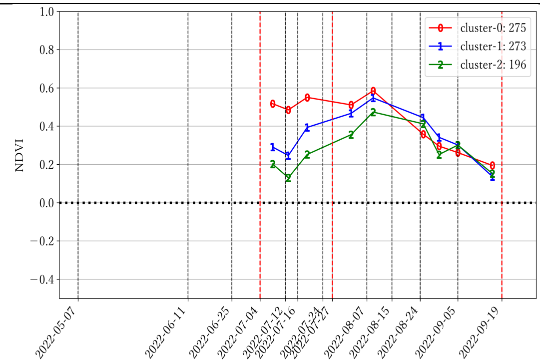	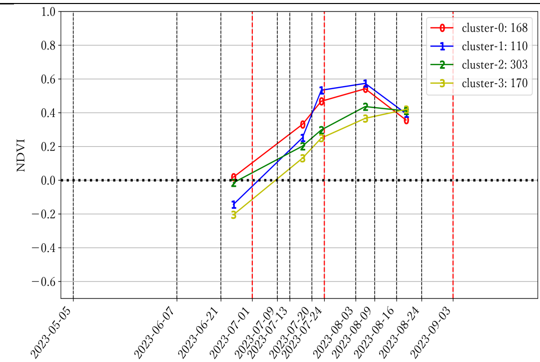	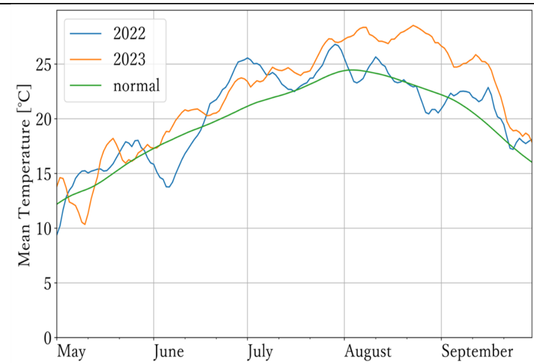
NDRE	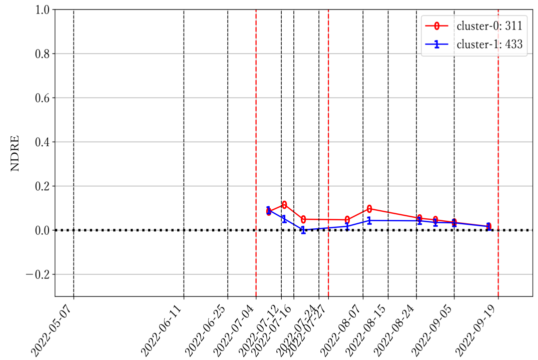	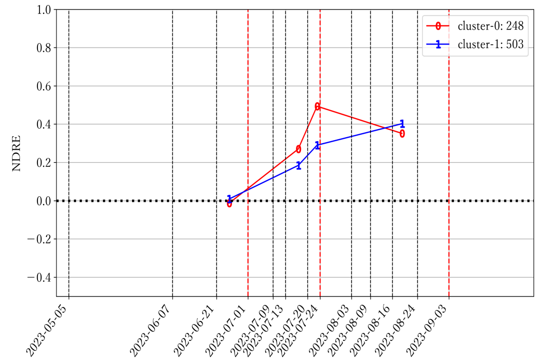	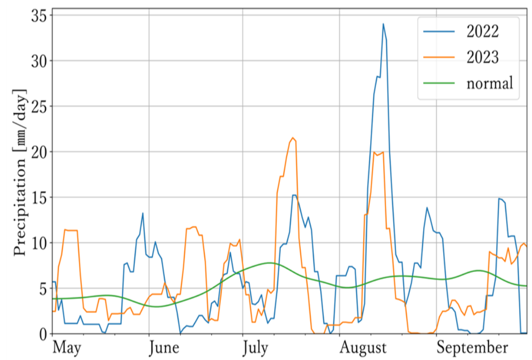
SNDRE	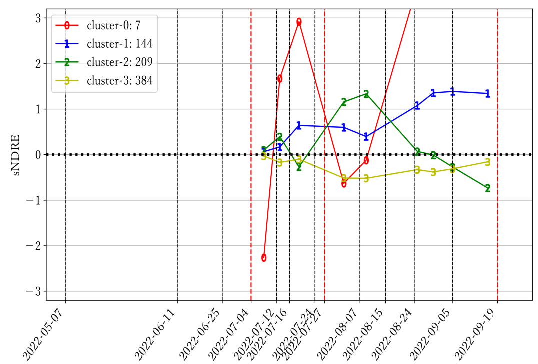	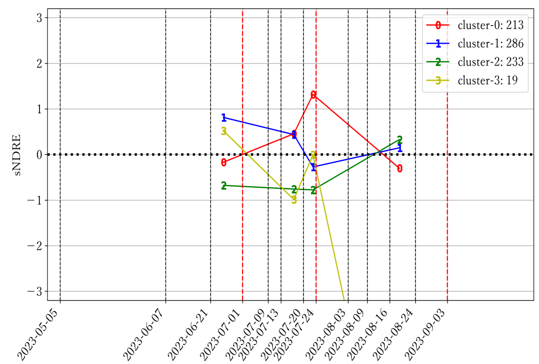	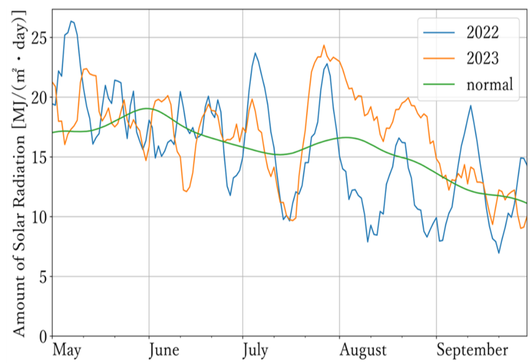

Table 3
Cluster distribution map

<table>
<tr><th>Year</th><th>2022</th><th>2023</th></tr>
<tr><td>NDVI</td><td>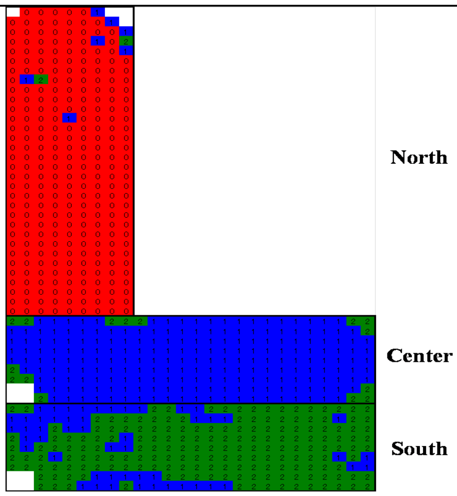
</td><td>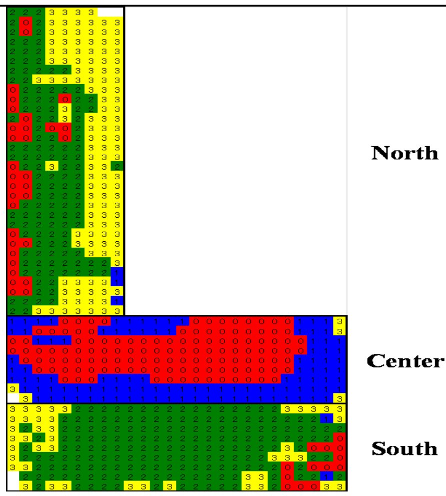
</td></tr>
<tr><td>NDRE</td><td>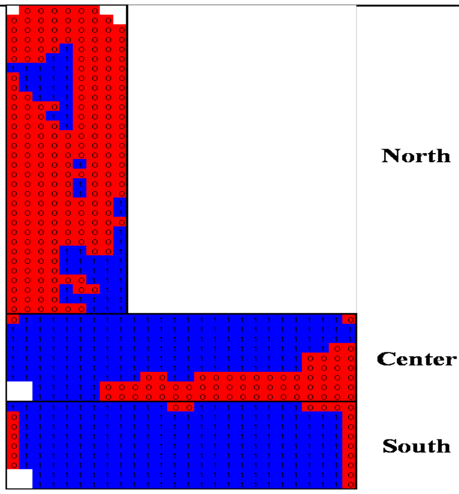
</td><td>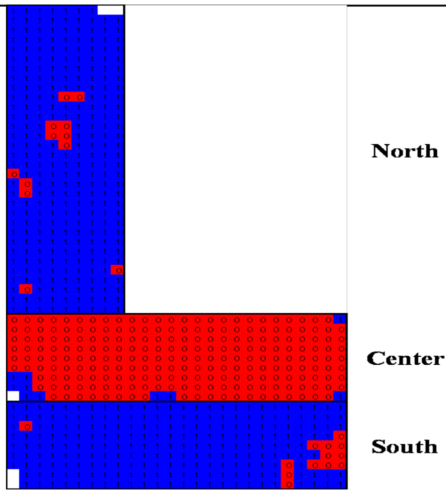
</td></tr>
<tr><td>SNDRE</td><td>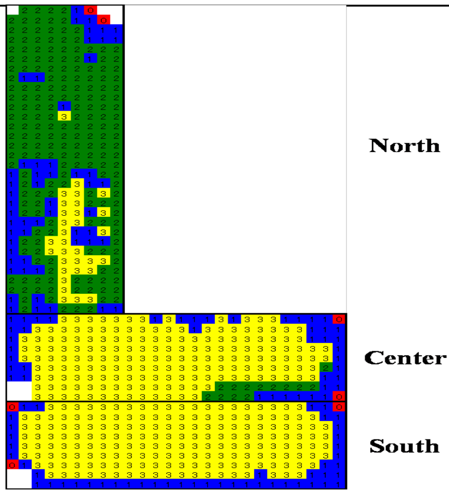
</td><td>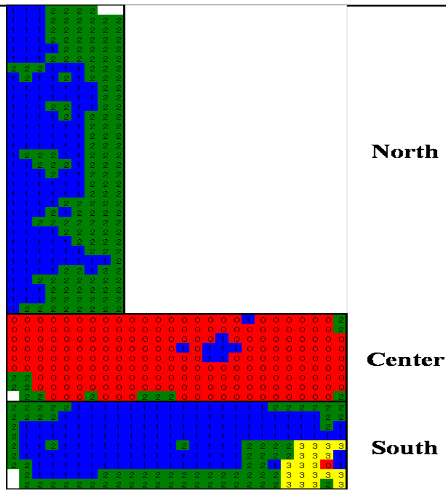
</td></tr>
</table>

3.2. Unit Acreage Sampling

The results of the unit acreage sampling are shown in Table 4. Each sample weighs 5 plants. "Average" row shows the average of that column converted into gram per unit area. In 2022, the average yield of Center field was higher and the average yield of South field was lower. This was consistent with the diagnosis from the time-series analysis. In 2023, the Center field had a higher yield than other fields by more than 40g/m². This was in line with the diagnosis from the time-series analysis. In addition, the sample data in 2022 was converted to “g/5plants” units and then a two-way analysis of variance was used to verify the significance of the average yields between years and paddy fields. In the results of this analysis, none of the factors showed any significant differences at the 5% level ($\text{p-value}_{\text{year}} = 0.488$, $\text{p-value}_{\text{field}} = 0.345$, $\text{p-value}_{\text{year}\times\text{field}} = 0.247$). Although there is no significant difference, the yield of North decreased largely in the high-temperature year. It has been reported that organic fertilizers tend to produce higher yields than chemical fertilizers, especially in years with abnormal weather [25, 26]. Chemical fertilizers are convenient because they are quick-acting. However, it is quickly absorbed by crops and weeds so is not as effective at improving soil fertility as organic fertilizers. To accurately measure the difference in effectiveness of different types of fertilizers, it seems necessary to improve the unit acreage sampling. Specifically, the sample size was too small (15 or 25 plants per paddy field), so the sampling method and sample size should be improved.

In both 2022 and 2023, the time-series analysis was conducted to diagnose which paddy fields could be properly fertilized. As a result of verifying this through the unit acreage sampling, the yield of well-diagnosed field was the highest in all cases. In other words, by time-series analysis of VIs using TSC, it was possible to evaluate the optimal fertilized fields. Also, the average yield differed by approximately 40g/m² in both years despite applying the same fertilizer to Center and the South fields. This is possibly caused by differences in soil properties. Center field had good drainage, and South field retains water well.

Table 4
Result of the unit acreage sampling

	2022 (g/3plants)			2023 (g/5plants)		
	North	Center	South	North	Center	South
Sample-1	70.8	132.4	86.0	133.4	150.0	133.0
Sample-2	82.0	79.6	86.8	155.5	143.4	140.3
Sample-3	80.6	84.8	78.2	106.9	129.1	135.6
Sample-4	94.2	68.2	84.6	131.1	165.4	137.1
Sample-5	89.6	76.4	73.2	116.8	136.0	121.2
Average [g/m^2]	505	534	495	467	526	484

4. Conclusion

Using the method of the previous research [18], this paper visualized additional fertilizer effects and high-temperature Influence. By grouping the VI time-series changes of each mesh using TSC, it was possible to visualize the growth and stress conditions, the effect of additional fertilizer, and diagnose which rice fields were fertilized properly. From the unit acreage sampling, all well-diagnosed rice field took the best yield. On the other hand, the yield of chemical fertilizer field decreased significantly in high-temperature years. Thus, under high-temperatures, it was suggested that organic fertilizers which improve soil fertility are more useful than chemical fertilizers which act fast.

To gain further insight, the following three things need to be considered. The first is to analyze images with wavelength bands not used in this study. Using green bands (GNDVI and so on) could visualize the water and nitrogen absorption. Using RGB images could provide ground truth data of soil and crops. The second is an improvement of the TSC algorithm. The K-Means++ method was used in this paper because it supported time-series data in Python. However, better classification can be expected by comparing with hierarchical clustering, DBSCAN, and so on. The third is to supplement missing data. When monitoring data cannot be obtained because the drone could not fly during rainy days, multiple imputation is considered a good approach.

Future works are creating target values for VIs for each growth stage to diagnose well conditions and predict yields. For the former, there is already research. This research makes NDVI target values to achieve the target yield by using a portable NDVI measuring device [27]. It is desirable to apply this to the UAV environment and to formulate target values for other VIs. The latter concerns preliminary evaluation. This research was an ex-post evaluation such as visualization of crop conditions and evaluation of additional fertilizer. However, in the future it is preferable to predict yields with fewer explanatory variables by weather data and growth stage prediction models. Furthermore, a system will need that outputs farm works support in natural language from such prediction models, VIs transitions, cluster maps, and so on. It is expected that UAV monitoring will become more widespread as research continues to meet the needs of the field.

References

[1] Japan Meteorological Agency, https://www.data.jma.go.jp/cpd/longfcst/extreme_japan/index.html, 2024. Accessed on 1 April 2024.

[2] Japan Meteorological Agency, https://www.jma.go.jp/jma/press/2401/04b/tenko2023.html, 2023. Accessed on 1 April 2024.

[3] Ministry of Agriculture, Forestry and Fisheries, https://www.maff.go.jp/j/tokei/kekka_gaiyou/sakumotu/sakkyou_kome/suiriku/r5/syukaku/, 2023. Accessed on 1 April 2024.

[4] Ministry of Agriculture, Forestry and Fisheries, https://www.maff.go.jp/j/seisan/syoryu/kensa/kome/attach/pdf/index-37.pdf, 2024. Accessed on 1 April 2024.

[5] Ministry of Agriculture, Forestry and Fisheries, https://www.maff.go.jp/j/kanbo/smart/#pro, 2023. Accessed on 5 April 2024.

[6] T. Ito, K. Minamino, S. Umeki, Analysis of vegetation indices by time series clustering of drone rice monitoring data, in: 3rd International Symposium on Electrical, Electronics and Information Engineering (ISEEIE 2023), volume 2023, IET, 2023, pp. 1–6.

[7] T. Ito, K. Minamino, S. Umeki, Analysis of fertilization effects on rice and wheat by time-series clustering of vegetation index data., in: ATAIT, 2023, pp. 55–65.

[8] C. HONGO, T. KOBAYASHI, Y. ARITA, The response of water status in tree seedlings through spectral reflectance, Journal of the Japan society of photogrammetry and remote sensing 37 (1998) 43–50.

[9] K. MIYAMA, Spectral reflection characteristics of crops and soil: Applicability of remote sensing technology to agricultural land survey, Journal of the Agricultural Engineering Society 56 (1988) 1197–1202.

[10] Y. INOUE, G. MIAH, E. SAKAIYA, K. NAKANO, K. KAWAMURA, Ndsi map and ipls using hyperspectral data for assessment of plant and ecosystem variables—with a case study on remote sensing of grain protein content, chlorophyll content and biomass in rice—, Journal of the Remote Sensing Society of Japan 28 (2008) 317–330.

[11] J. Xue, B. Su, Significant remote sensing vegetation indices: A review of developments and applications, Journal of sensors 2017 (2017) 1353691.

[12] The IDB Project, https://www.indexdatabase.de/, 2024. [Accessed on 6 April 2024].

[13] S. Guan, K. Fukami, H. Matsunaka, M. Okami, R. Tanaka, H. Nakano, T. Sakai, K. Nakano, H. Ohdan, K. Takahashi, Assessing correlation of high-resolution ndvi with fertilizer application level and yield of rice and wheat crops using small uavs, Remote Sensing 11 (2019) 112.

[14] H. Zheng, W. Ji, W. Wang, J. Lu, D. Li, C. Guo, X. Yao, Y. Tian, W. Cao, Y. Zhu, et al., Transferability of models for predicting rice grain yield from unmanned aerial vehicle (uav) multispectral imagery across years, cultivars and sensors, Drones 6 (2022) 423.

[15] T. K. Wardana, Y. Arkeman, K. Priandana, F. Kurniawan, et al., Use of plant health level based on random forest algorithm for agricultural drone target points, Jurnal RESTI (Rekayasa Sistem dan Teknologi Informasi) 7 (2023) 637–645.

[16] K. Tanaka, A. Kondoh, Mapping of rice growth using low altitude remote sensing by multicopter, Journal of the Remote Sensing Society of Japan 39 (2019) S1–S17.

[17] K. Harashina, K. Yamamoto, M. Maki, Y. Muto, E. Kurashima, Monitoring growth of water-seeded rice in tsunami-stricken paddy fields using uav-mounted multispectral sensor, Journal of the Japanese Society of Irrigation, Drainage and Rural Engineering 87 (2019) 121–126.

[18] T. Ito, Lower Costs and Environmental Loading Reduction of Agriculture by Time-series Analysis of Vegetation Indices Using Drones, Master's thesis, Iwate Prefectural University, Takizawa, 2024.

[19] S. Sato, T. Ito, S. Umeki, K. Minamino, Analysis of the impact of high temperatures on paddy rice using drone monitoring and time-series clustering, in: The 86th National Convention of IPSJ, Yokohama, 2024.

[20] DJI Co., Ltd., https://www.dji.com/jp/p4-multispectral, 2024. [Accessed 6 April 2024].

[21] QGIS Development Team, https://www.qgis.org/en/site/, 2024. [Accessed 6 April 2024].

[22] C. Shi, B. Wei, S. Wei, W. Wang, H. Liu, J. Liu, A quantitative discriminant method of elbow point for the optimal number of clusters in clustering algorithm, EURASIP journal on wireless communications and networking 2021 (2021) 1–16.

[23] E. Kanda, Y. Torigoe, T. Kobayashi, A model to estimate the increase of leaf number on the main culm of the rice plant, Japanese Journal of Crop Science 69 (2000) 540–546.

[24] E. Kanda, Y. Torigoe, T. Kobayashi, A simple model to predict the developmental stages of rice panicles using the effective accumulative temperature (modelling, information technology and environment), Japanese Journal of Crop Science 71 (2002) 394–402.

[25] Warm region global warming research team, Kyushu/Okinawa branch, NARO, 2007. URL: https://www.naro.affrc.go.jp/org/karc/seika/kyushu_seika/2007/2007041.html, [Accessed 9 May 2024].

[26] Current status and direction of cultivation technology development compatible with high temperatures, Memoirs of the National Agricultural Research Center for Kyushu Okinawa Region 94 (2010) 71–93.

[27] Y. Kaneta, M. Nishida, F. Takakai, T. Sato, New growth diagnosis standards of high-yielding rice and demonstration of high yielding using ndvi by greenseeker handheld crop sensor, Journal of the science of soil and manure 91 (2020) 417–425.